International Journal of Nanomedicine

Dovepress
open access to scientific and medical research

Open Access Full Text Article

ORIGINAL RESEARCH

Design, Formulation and in vivo Evaluation of Novel Honokiol-Loaded PEGylated PLGA Nanocapsules for Treatment of Breast Cancer

This article was published in the following Dove Press journal:
International Journal of Nanomedicine

Yusuf A Haggag[1]
Rowida R Ibrahim[2]
Amin A Hafiz[3]

[1]Department of Pharmaceutical Technology, Faculty of Pharmacy, Tanta University, Tanta, Egypt; [2]Medical Biochemistry and Molecular Biology Department, Faculty of Medicine, Tanta University, Tanta, Egypt; [3]Department of Clinical Nutrition, Faculty of Applied Medical Sciences, Umm Al-Qura University, Mecca, Kingdom of Saudi Arabia

Background: Honokiol (HK) is a common herbal medicine extracted from magnolia plants. Low aqueous solubility and limited bioavailability of HK have hindered its clinical application, especially for cancer treatment. Nano-drug delivery system has the potential to enhance HK delivery and therefore, enhance its anti-cancer activity.

Purpose: The study's aim is to design novel PEGylated-PLGA polymeric nanocapsules (NCs) for HK delivery to breast tumor-bearing mice after systemic administration.

Methods: Formulation of different HK-loaded NCs and their physio-chemical characterization were optimized through the use of different formulation variables. The antitumor activity of the HK-loaded NCs was investigated both in vitro using MCF-7 and EAC breast cancer cell lines and in vivo using solid Ehrlich carcinoma (SEC) breast cancer model.

Results: The optimum HK-loaded NCs were prepared from 15% PEG-PLGA diblock copolymer and exhibited the lowest nano size of 125 nm, smooth spherical morphology, highest drug loading of 94% and highest cellular uptake into breast cancer cells. HK-loaded PEGylated NCs can effectively inhibit the in vitro cell growth of breast cancer cells by 80.2% and 58.1% compared to 35% and 31% with free HK in the case of MCF-7 and EAC, respectively. HK-loaded NCs inhibited SEC tumor growth by 2.3 fold significantly higher than free HK, in vivo.

Conclusion: The designed drug delivery system encapsulating HK exhibited a pronounced decrease in tumor growth biomarkers meanwhile proved its safety in animals. Therefore, 15% PEGylated HK-loaded NCs may act as a promising new approach for breast cancer treatment.

Keywords: honokiol, nanocapsule, PEG-PLGA copolymers, formulation variables, anti-cancer activity, solid Ehrlich carcinoma, breast cancer

Introduction

Breast cancer is the most common type of cancer and the second leading reason for cancer-related mortality in females. Recently, American Cancer Society annual estimates for breast cancer showed that approximately 268,600 new cases of invasive breast cancer, 62,930 of early breast cancer new cases will be diagnosed in American women and about 41,760 females will die from breast cancer during this year. Despite major advances in screening programs and treatment protocols, one from every eight women will develop breast cancer.[1] Therefore, more-effective therapeutic approaches are critically needed to decrease morbidity and to combat breast cancer.[2]

Correspondence: Yusuf A Haggag
Department of Pharmaceutical Technology, Faculty of Pharmacy, Tanta University, Tanta 31111, Egypt
Tel +2 01220104612
Fax +2 040 3335466
Email youssif.hagag@pharm.tanta.edu.eg

submit your manuscript | www.dovepress.com
DovePress
http://doi.org/10.2147/IJN.S241428

Honokiol is a bioactive polyphenol extracted from Magnolia species which has been commonly used in China and Japan as an herbal medicine.[3] It is well known for its wide pharmacological activity as it possesses anti-cancer, anti–viral, anti–inflammatory, antioxidant, antithrombotic and neurological effect.[3–7] Besides, HK is considered as a natural peroxisome proliferator-activated receptor gamma (PPARγ) agonist that can be used clinically to control hyperglycemia and its unfavorable side effects, such as weight gain.[8] Although honokiol can be used for the treatment of all previous diseases, its poor aqueous solubility is the major hurdle against its therapeutic applicability. Therefore, it is essential to design a proper drug delivery system to improve HK solubility and hence its bioavailability and therapeutic efficacy.

Nanotechnology has achieved major progress in the design, synthesis, and development, of different forms of nanosystems to fulfill different drug purposeful applications. Polymeric nanoparticles as a type of colloidal dispersions have been studied for the delivery of bioactive drugs either in pharmaceutical or biotechnological field.[9–12] Among the different polymeric nanoparticles used, nanocapsules have attracted increased attention.[13,14] Their advantages over classical drug delivery systems are numerous, as they can enhance the aqueous solubility of lipophilic drugs, control its release and increase the bioavailability of different drugs.[14–16] In addition, nanocapsule-base drug delivery systems were effectively used in cancer treatment due to its biodegradability, high drug-loading capacity, high cellular uptake, preferable intra-tumor bio-distribution and possible functionalization for cancer targeting.[14]

Polymeric nanocapsule encapsulating lipophilic drugs generally consists of polymeric shell and an oily core containing dissolved drug. Therefore, the use of appropriate biodegradable and biocompatible polymers like poly (lactide-co-glycolide) (PLGA), polylactic acid (PLA) and poly (ε-caprolactone) (PCL) is commonly adopted in formulation of NCs.[13] PEGylated PLGA and PCL diblock copolymers have emerged as a fascinating class of drug delivery polymers for biomedical and drug delivery applications.[17–19] These polymers are sufficiently stable in vitro and long-circulating in vivo besides they showed high cancer cell internalization by Enhanced Penetration Retention (EPR) effect to achieve passive targeting to tumor site.[12,20]

Several attempts are described to develop different carrier-mediated drug delivery strategies for HK based on nanotechnology. These nano-drug delivery systems include nanosuspension,[21] nanoparticles,[22–24] microbubbles,[25] liposomes[26] and polymeric micelles.[27,28] Recently, very few studies tried quantum dots-based nanocapsules for co-delivery of honokiol and other anti-cancer drugs for theranostic applications.[29,30]

This is the first paper to report the formulation of PEGylated PLGA NCs encapsulating honokiol. To our knowledge, no studies so far have investigated the anti-cancer potential of HK-loaded PEGylated PLGA NCs for treatment of the Solid Ehrlich Carcinoma breast cancer model in vivo after systemic administration.

The objective of this study is to design biocompatible HK-loaded PEGylated PLGA NCs for breast cancer treatment. The first aim was to adjust various formulation parameters, such as the PEG content in the polymeric backbone and the type of the oily core, in order to optimize the physio-chemical properties of HK-loaded NCs. The second aim was to investigate cellular delivery and in vitro cytotoxicity of HK NCs using two different breast cancer cell lines of MCF-7 and EAC. The last aim is to study the anti-tumor activity and safety profile of optimum HK-loaded NC in vivo using the SEC breast cancer model.

Materials and Methods

Materials and Reagents

PEG-PLGA diblock copolymers (Resomer® RGP d 50155 (15% PEG of MW 5 kDa)) Resomer® RGP d 50105 (10% of PEG, MW 5 kDa) and Resomer® RGP d 5055 (5% PEG of MW 5 kDa) were purchased from Boehringer Ingelheim Ltd. (Ingelheim, Germany). Honokiol, coumarin 6, dialysis tubing (MWCO 2000 Da), SP-Sephadex C-25 resin, almond oil, castor oil, isopropyl myristate, soybean lecithin, tween 80, acetone, absolute ethanol (ultra-pure grades) were purchased from Sigma Chemical Co. (St. Louis, USA). Dulbecco's modified Eagle's medium (DMEM) media, trypsin/EDTA, phosphate-buffered saline (PBS), fetal bovine serum (FBS), and penicillin/streptomycin were obtained from Gibco, Invitrogen, UK.

MCF-7 breast cancer cell line was obtained from the Cell Culture Department, VACSERA (Cairo, Egypt). Cells were routinely grown in T75 canted-neck tissue culture flasks. Cells were cultured in low glucose DMEM media supplemented with FBS (10% v/v), L-glutamine (2 mmol L^{-1}), penicillin (100 U mL^{-1}) and streptomycin (100 μg mL^{-1}). Medium renewal was done every three days at 80% confluence. Cell cultures were incubated at conditions of 5% CO_2 and 37°C. Ehrlich Ascites Carcinoma cell line (EAC) was obtained from Experimental Oncology Unit of the National Cancer Institute (NCI) (Cairo University, Cairo, Egypt) was

maintained by weekly intraperitoneal transplantation of respective tumor cells (2×10^6 cells per mouse) in stock animals.

Preparation of HK-Loaded Polymeric NCs

Screening Solubility of HK in Different Oils

The practical solubility of HK in different oils used for NCs preparation (almond oil, castor oil, or isopropyl myristate) was determined by the shake-flask saturation method.[14] Excess amount of HK (5 mg) was placed in glass vials containing 1 mL of the (almond oil, castor oil, or isopropyl myristate), sealed and shaken at 100 rpm for two days at 37°C. After centrifugation, an aliquot from the supernatant was withdrawn and mixed with acetone and ethanol mixture (1:1 v/v). The solubility of HK in different oils was determined by using a UV spectrophotometer (Model UV-1601 PC; Shimadzu, Kyoto, Japan) and measuring the absorbance at 294 nm.[24] The amount of soluble HK was estimated according to relevant standard plots. Standard plots were obtained after testing the solubility of five different concentrations of HK (0.1, 0.2, 0.4, 0.6 and 0.8 mg/mL) in each oil type separately. Each HK concentration was treated as previously mentioned and the UV absorbance was measured. A linear relationship was plotted between absorbance and HK concentration.

Formulation of HK-Loaded NCs

HK-loaded NCs were prepared by the nanoprecipitation method as described by[31] with some modifications. The oily phase composed of 50 mg of polymer (5% PEG-PLGA, 10% PEG-PLGA or 15% PEG-PLGA diblock copolymers), 5 mg of HK, 25 mg of soybean lecithin and 500 µL of oil (almond oil, castor oil, or isopropyl myristate) dissolved in 5 mL of acetone/ethanol (1:1 v/v) mixture. This oily phase was added dropwise into 10 mL of aqueous phase containing 0.2% of Tween 80. The final mixture was kept under magnetic stirring for 60 min to facilitate organic solvent diffusion and formation of NCs. Elimination of organic solvents was done using a rotary evaporator under reduced pressure then lyophilized using Freeze-dryer (Crydos-50, Telstar, Spain). Coumarin 6 labeled NCs were prepared according to the previous steps with only one modification by adding coumarin 6 (100 µg) to the oily phase. Fluorescent HK-loaded NCs were also evaluated with respect to, particle size, polydispersity index (PDI) and zeta potential. Process variables, such as PEG content in the polymeric backbone and type of the oily core are listed in Table 1, with the identifying code for each HK-loaded NC formulation.

Physicochemical Characterization of HK-Loaded NCs

The mean particle size and particle size distribution of HK-loaded NCs were determined depending on the Dynamic Light Scattering technique (Zetasizer 5000, Malvern Instruments, Malvern, UK). HK-loaded NCs suspension was prepared by dispersing lyophilized-powder into ultrapure water, a liquid sample was further diluted and the average of three measurements was recorded. Another aliquot of colloidal suspensions was diluted in aqueous 0.001 M KCl solutions to adjust the sample conductivity, and Laser Doppler Anemometry (Zetasizer 5000, Malvern Instruments, Malvern, UK) was used to measure the zeta potential of HK-loaded NCs. NP surface morphology was studied using Transmission Electron Microscopy (JOEL JEM 2000 EX200) operating at an accelerating voltage of 80 kV. Liquid samples were placed on a formvar-coated grid with evaporated carbon for drying before scanning.

Determination of HK Encapsulation Efficiency (%E.E)

The encapsulation efficiency (%E.E) of HK-loaded NCs was determined by the indirect method. Firstly, the purification of NC samples to remove the un-entrapped drug was done by using a PD10 desalting column (GE Healthcare) with Tris buffer and purified fractions were collected. Secondly, the amount of non-encapsulated HK in the supernatant after purification of NCs suspension was determined by high-performance liquid chromatography technique (HPLC) according to the previously reported

Table 1 Process Variables for HK-Loaded NCs and Corresponding Identifiers

Formulation Identifier	Polymer Type	Oily Core
F1	5%PEG-PLGA	Almond oil
F2	5%PEG-PLGA	Castor oil
F3	5%PEG-PLGA	Isopropyl myristate
F4	10%PEG-PLGA	Almond oil
F5	10%PEG-PLGA	Castor oil
F6	10%PEG-PLGA	Isopropyl myristate
F7	15%PEG-PLGA	Almond oil
F8	15%PEG-PLGA	Castor oil
F9	15%PEG-PLGA	Isopropyl myristate

method.[24] 100 µL of the NCs preparations were diluted by the mobile phase. The amount of free HK was analyzed using HPLC equipment (Waters® C18-5 column mm, 5 µm). The composition of the mobile phase was methanol, acetonitrile, and water (55:20:25, v/v/v) at a flow rate of 1 mL min^{-1}. The injection volume was 40 µL and the wavelength for UV detection was 294 nm.

In vitro Release Profile

A sample of HK-loaded NC formulation containing a predetermined amount of HK was placed into a 10 kDa dialysis bag. The dialysis membrane containing HK-loaded NCs was agitated at 100 rpm in a receptor media composed of 50 mL PBS (pH 7.4) containing tween 80 (1% w/v) at 37°C. At predetermined time interval points, 1 mL sample was withdrawn and replaced by an equal fresh volume of the same media at 37°C to maintain sink conditions.[14] The same amount of HK was dissolved in DMSO and placed into the same dialysis bag for release comparison. This control experiment was set up to ensure the presence of sink conditions and the absence of non-specific adsorption of HK to the dialysis membrane. HK concentration was assessed by HPLC method as previously reported.[24]

In vitro Stability

HK-loaded NC preparations were sealed in glass vials and stored in the desiccator at room temperature of 25°C. The stability of HK-loaded NC lyophilized-powders (F1, F4, and F7) was tested every time intervals of 0, 2, 4 and 6 months after preparation to determine the sample size, PDI, zeta-potential and % E.E of NC formulations. Each sample was tested three times and the average of three different measurements was presented.

Seeding of MCF-7 and EAC Cancer Cell Lines

MCF-7 human breast cancer cells were harvested, when they are 90% confluent, and the cell suspension was centrifuged at 1200 rpm (4°C) for 5 mins for cell precipitation. The cell pellets were resuspended in DMEM complete growth medium. EAC cells were obtained from the ascites fluid of BALB/C mice bearing 8–10 days induced ascites tumor. EAC was suspended in PBS before treatment. Cell count was performed on a 10 µL cell sample using a Neuberger hemocytometer.

Cellular Uptake of HK-Loaded NCs

Cellular uptake of coumarin 6-tagged HK-loaded NCs (F1, F4, and F7) into MCF-7 cell line was evaluated using flow cytometry and confocal laser scanning microscopy.[11,13] Briefly, for flow cytometry analysis, treatment with either coumarin 6 solutions or coumarin 6 labeled HK NCs was suspended in Optimem® media and added to MCF-7 cells for 24 hrs in 6-well plates. Cells were collected by trypsinization then treated with FACS buffer. Cellular uptake of HK-loaded NCs was quantified by gating cells for positive coumarin 6 fluorescence and results were analyzed using BD FACS Calibur flow cytometer (BD Biosciences). Three independent experiments were used for measurements and cellular uptake values were calculated as mean ± SD. Cellular localization of Coumarin 6-tagged HK-loaded NCs was evaluated qualitatively by confocal laser microscope (Carl-ZEISS Cell Observer, Confocal Microscope, LSM-710, Germany). Coumarin 6-tagged HK-loaded NCs fluorescence was observed by using a 456-nm excitation filter and emission wavelength of ($\lambda Em = 500$ nm). Intracellular localization of fluorescent NCs into MCF-7 cells was detected one day after treatment. Briefly, MCF-7 cells were seeded into a 6-well plate, containing two fixed coverslips incubated into 2.0 mL of DMEM growth medium. Coverslips were mounted using mounting media and counterstained with DAPI. Cellular localization of labeled NCs was represented by the green fluorescence, while cell nuclei were demonstrated by blue fluorescence signals. Untreated MCF-7 cells and cells treated with free coumarin 6 were included as negative and positive controls, respectively.

In vitro Cell Viability Assay

MCF-7 breast cancer cell line was seeded in 24-well plates and incubated with 0.5 mL of complete growth media. After 24 h, cells were treated with blank NCs, free HK or HK-loaded NCs (F7) with different concentrations (5, 10, 20 µM). Cytotoxicity was examined by MTT assay as previously reported by.[11,20] After treatment with 24, 48 and 72 h, media was removed and cells were treated by 500 µL of (15% v/v MTT solution). MCF-7 cells were incubated at 37°C and 5% CO_2 for 3 h. Afterward, formazan crystals formed were dissolved in DMSO (500 µL) and the plate was read at 570 nm in an FLUO star Omega microplate reader (BMG Labtech) and the results were expressed as the cell viability after treatment was compared to control cell viability. The viability of EAC cells

after treatment with different concentrations of free HK and HK-loaded NCs (F7) (5, 10, 20 μM) was tested by trypan blue exclusion assay as previously reported by.[32,33] Briefly, 2.5 × 10^5 cell/mL of EAC cells was resuspended in PBS and incubated for 3 h at 37°C. At the end of the incubation period, an equal volume of trypan blue dye solution was added to cell samples, and afterward, the unstained alive cells and stained dead cells were counted using a hemocytometer. The percent of cell viability for each test was calculated.

In vivo Study

Animals

Thirty-two female Swiss albino mice (18–20 g) were fed water and standard pellet chow (EL-Nasr Chemical Company, Cairo, Egypt) ad libitum for the whole duration of the in vivo experiment. The in vivo study was performed in accordance with the guide of the National Institutes of Health about the use and care of laboratory animals (NIH Publications No. 8023, revised 1978) and approved by Tanta University Animal Ethical Committee, Egypt. Mice were housed and allowed to acclimatize to laboratory conditions for 7 days prior to the experiment. The cell viability of EAC cells aspirated from the mice peritoneal cavity was adjusted to be 98% as calculated from the trypan blue exclusion assay. A xenograft model of Solid Ehrlich Carcinoma (SEC) was induced in female Swiss albino mice by subcutaneous implanting of 2×10^6 viable EAC cells suspended in 200 μL of saline in the right thigh of each mouse. The tumor developed as a palpable solid tumor mass which was achieved within 12 days post-implantation in all mice.[12,20]

In vivo Anti-Tumor Activity

The antitumor activity of HK-loaded NC was evaluated in vivo using mice, bearing a solid tumor of mammary origin. Mice rendered tumor-bearing were divided randomly into 4 groups, each containing 8 animals. Animals served as the control group received saline as an intraperitoneal injection. A volume of 0.2 mL of HK-NCs suspension was injected into the lower right quadrant of mice abdomen using 25g needle gauge after disinfection of the abdominal area with alcohol. The first treated group was given blank NCs and the second treated group was given an intraperitoneal administration of frees HK at a dose of 15 mg kg^{-1}. The last treated group was injected by HK-loaded NP (F7) at the same dose. All treatments were injected every three days with a total of 5 injections during the whole experiment. The treatment protocol for all groups was started on day 13 and extended to the 30th-day post-implantation. Tumor volumes were recorded from the start point of the treatment and thereafter every 2 days till the last measurement taken at the 17th day of treatment and just prior to the sacrifice of surviving animals. A digital Vernier caliper was used to record dimensions (mm) and the following formula was applied to calculate the volume of the developed tumor mass;[34]

$$\text{Tumor volume}\left(\text{mm}^3\right) = 0.52.\text{length.width}^2$$

Drug efficacy was calculated by the percentage of tumor growth inhibition as previously reported by.[35] After finishing the experiment, all animals were sacrificed after being anesthetized with ether and blood was withdrawn into a complete dry sterile centrifugation tubes, left to clot at room temperature for 30 min, centrifuged (1000 g) for 20 min at 4°C. Serum was separated, collected and stored at −20°C for further biochemical analysis. Implanted tumors were excised to be weighed. The changes in tumor weights for each animal group were recorded.

ELISA Assay for Tumor Growth Biomarkers

At the endpoint of the experiment, excised tumor tissue was homogenized in a Potter–Elvenhjem tissue homogenizer using ice-cold 50mM PBS with adjusted pH 7.4, containing 1.15% KCl. Next homogenates were centrifuged (10,000 g) at 4°C for 20 min. The cell debris pellets were discarded while the supernatants were collected, divided into aliquots and stored at −80°C for quantitative estimation of tumor growth biomarkers. Biomarkers as vascular endothelial growth factor (VEGF), Caspase-3 and Bcl-2 were measured using ELISA kit purchased from (Sunred Biological Technology Co. Ltd, China) according to manufacturer's protocols.

Evaluation of in vivo Toxicity of HK-Loaded NCs

After Mice were sacrificed, organs like heart, liver, spleen, lung, and kidneys were excised and accurately weighed. The immune organ index was determined according to the following formula.[24]

$$\text{Immune organ index} = \text{Weight of immune organs(g)} / \text{Bodyweight(g)}$$

Serum samples extracted from all animals were analyzed for evaluating aspartate aminotransferase (AST) and alanine aminotransferase (ALT) calorimetrically at wavelength of 340nm using (BioSystems, Egypt kits) to assess hepatic damage. Serum creatinine levels, an indicator for possible

renal damage, were assayed by spectrophotometry at 490 nm with an enzymatic–colorimetric method using commercially available kits supplied by (Biodiagnostic, Egypt). Blood biochemistry was examined for the control group, free HK treated and HK-loaded NCs (F7) treated groups and compared with each other.

Statistical Analysis

Results for in vitro experiments were demonstrated as mean ± SD and results from in vivo experiment, were presented as mean ± SEM. Significant differences were evaluated statistically using one-way ANOVA followed by post-hoc Tukey's test. $P < 0.05$ was considered to be statistically significant for both in vitro and in vivo experiments.

Results and Discussion

Solvent displacement technique also called nanoprecipitation is the most applicable method for polymeric NCs preparation. It has been successfully used for entrapment of different lipophilic drugs and other bioactive molecules.[16] The advantages of this quick methodology are the production of smaller size nanoparticles less than 200 nm with a homogenous size distribution, high drug-loading capacity and long-term stability. Another advantage is no need for high shearing force, sonication, or high temperatures which is essential in the case of sensitive bioactive molecules.[36]

Effect of PEG Content of the Polymer Backbone

The physicochemical properties of three different formulations of HK-loaded NCs (F1, F4, and F7) made from different diblock copolymers depending on the PEG content were presented in (Figure 1). HK-loaded 15% PEG-PLGA NCs (F7) were significantly smaller in size than F1 ($p < 0.001$, n=3) and F4 ($p < 0.05$, n=3) prepared from 5% to 10% PEG-PLGA diblock copolymer, respectively. Increasing the concentration of PEG in the polymeric backbone caused a decrease in the nanoparticles' size

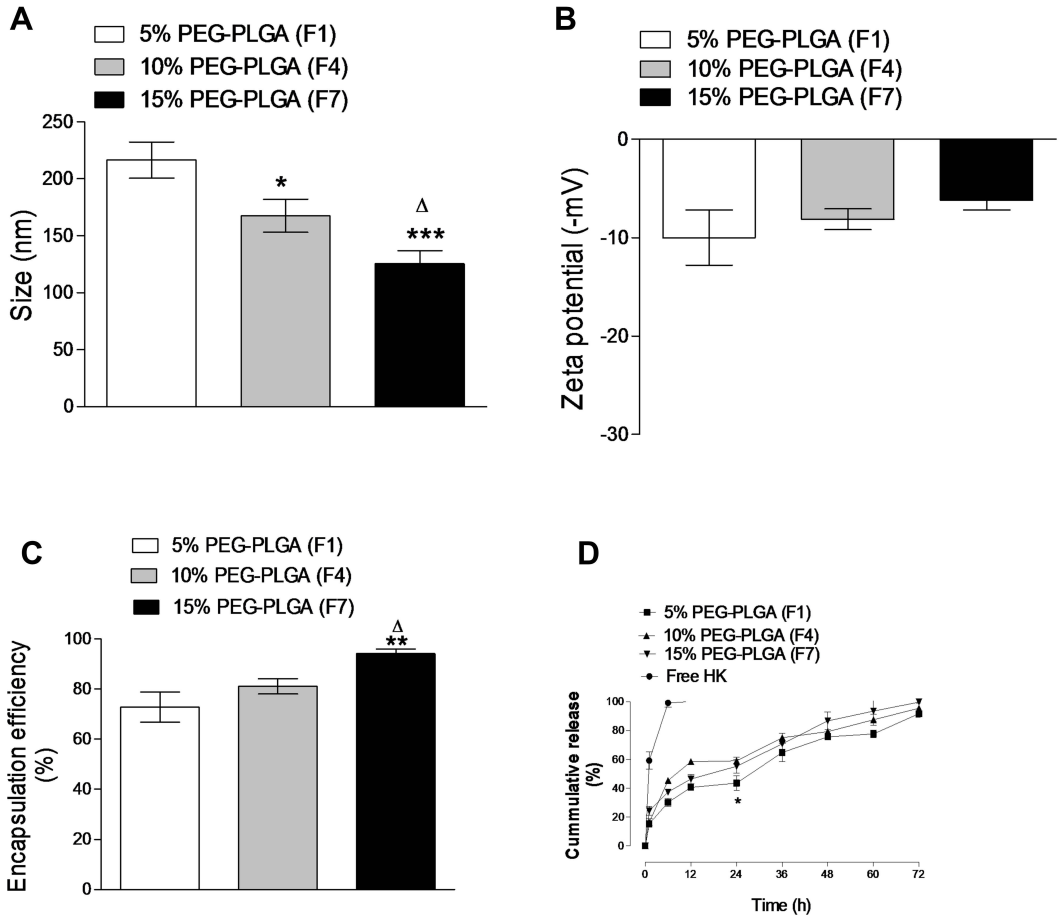

Figure 1 Effects of PEG content of the polymer backbone on NCs size (**A**), zeta potential (**B**), encapsulation efficiency (**C**) and HK in vitro release (**D**). Values are mean ± SD for (n = 3). For (**A**–**C**), *p < 0.05, **p < 0.01, ***p < 0.001 compared with 5% PEG-PLGA (F1). $^{\Delta}p < 0.05$ compared with 10% PEG-PLGA (F4).

with the largest size for F1 prepared from 5% PEG-PLGA (Figure 1A). Increasing PEG content led to the formation of a shorter chain length of diblock copolymers. The particle size is increased by an increase in the hydrophobic segment,[37] which is a similar finding to that reported in other studies.[10,12] All NC formulations showed a low polydispersity index (PDI) values ranging from 0.21 to 0.32.

PEGylating, irrespective of PEG concentration, reduces the total negative surface charge of PLGA polymer. PEGylated PLGA NCs (F7) had a lower negative value of (−6.21 mV) compared to F1 and F4 ($p > 0.05$, n=3) (Figure 1B). The Presence of PEG as a non-ionic hydrophilic moiety decreases the zeta potential of PLGA polymer through masking a part of the polymer anionic charge which is responsible for the high negative surface charge values of PLGA polymer.[38]

HK loading and encapsulation efficiency were significantly increased by increasing the PEG concentrations in the polymer matrix. 15% PEGylated PLGA NCs (F7) showed a significant increase in HK encapsulation efficiency compared to F1 ($p < 0.01$, n=3) and F4 ($p < 0.05$, n=3) (Figure 1C). These results are attributed to the high amphiphilic property of 15% PEG-PLGA copolymer which facilitate micelle formation in addition to the presence of high content of PEG chains which increases the surface area of the NCs and consequently increase the probability for a greater amount of drug to be loaded and thus increase its encapsulation efficiency.[18] Drug entrapment efficiency depends on different parameters such as drug solubility, matrix composition, drug–polymer interactions, and the presence of functional groups in either the drug or matrix.[11,39] PEG-PLGA is the polymer of choice for HK-NCs formulations as PEG, showed a pronounced effect on drug-loading and interactions.[18] High PEG content in case of 15% PEG-PLGA copolymer showed a higher rate of solidification compared to 5 and 10% PEG-PLGA copolymer due to lower solubility in the organic phase which finally lead to higher entrapment of HK after organic solvent evaporation to form drug-loaded NCs.[10]

In vitro release profile of (F1, F4 and F7) showed that the HK burst release after 24 h was faster and significantly higher form the F7 which released approximately 55.24% of HK compared to 43.53% released from the F1 ($p < 0.05$, n=3) however non-significant difference was observed in case of F4 ($p > 0.05$, n=3) (Figure 1D). Burst release phenomenon can be attributed to the drug attached to the surface of the NCs.[40] Moreover, PEG chains are hydrophilic and can be easily dissolved in an aqueous release medium which derived the water to penetrate into the oily core, allowing HK to be released. Higher content of PEG accelerated the degradation rate because it facilitates higher water penetration compared with other NCs.[41] The in vitro release profile of HK/DMSO control showed a 100% drug release achieved within the first 6 h which indicates satisfying the sink conditions besides the absence of non-specific drug absorption to the dialysis membrane. Moreover, this release profile can confirm the sustained drug release from nanocapsules compared to the control drug.

Effect of Type of Oily Core

PEGylated NCs encapsulating HK were formulated using one of the following oils (almond oil, castor oil or isopropyl myristate). HK showed its lowest solubility in isopropyl myristate (0.99 mg mL^{-1}) which was significantly lower than castor oil (1.81 mg mL^{-1}) ($p < 0.05$, n=3). The highest HK solubility was achieved in almond oil (2.56 mg mL^{-1}), at 37°C ($p < 0.01$, n=3). HK-loaded 15% PEGylated NCs based on isopropyl myristate (F9) exhibited significantly bigger size (177.5 ± 15.4 nm) compared to NC prepared from castor oil (F8) (166.5 ± 11.23) ($p < 0.01$, n=3) and NC prepared from almond oil (F7) (125.5 ± 11.5) ($p < 0.05$, n=3). A similar pattern was observed in the case of 5% PEG-PLGA NCs; however, this behavior was not the same in the case of 10% PEG-PLGA NCs (Figure 2A). The PDI value in the case of NCs prepared from almond oil as an oily core was significantly lower than other PDI values for isopropyl myristate and castor oil NCs indicating more homogenous size distribution.

The type of oil has no significant effect on the ζ-potential of different NCs formulations ($p > 0.05$, n=3) (Figure 2B). The encapsulation efficiency of all HK-loaded NCs ranged from (58.89 ± 5.9 to 94.18% ± 1.8%). Almond oil-based NCs demonstrated significantly higher encapsulation efficiency values compared to castor oil and isopropyl myristate-based formulation regardless of the type of the polymer ($p < 0.05$, n=3) (Figure 2C). This is might be attributed to the highest solubility of HK in almond oil which prevents its loss towards the aqueous phase leading to higher drug entrapment inside the oily core. Moreover, almond oil has a lower hydrophilic-lipophilic balance (HLB 6), than castor oil (HLB 14) and isopropyl myristate (HLB 11.5); therefore, the nanocapsules based on almond oily core will be more suitable for HK loading due to its high lipophilicity.[42] A similar finding was reported in previous studies.[13,14]

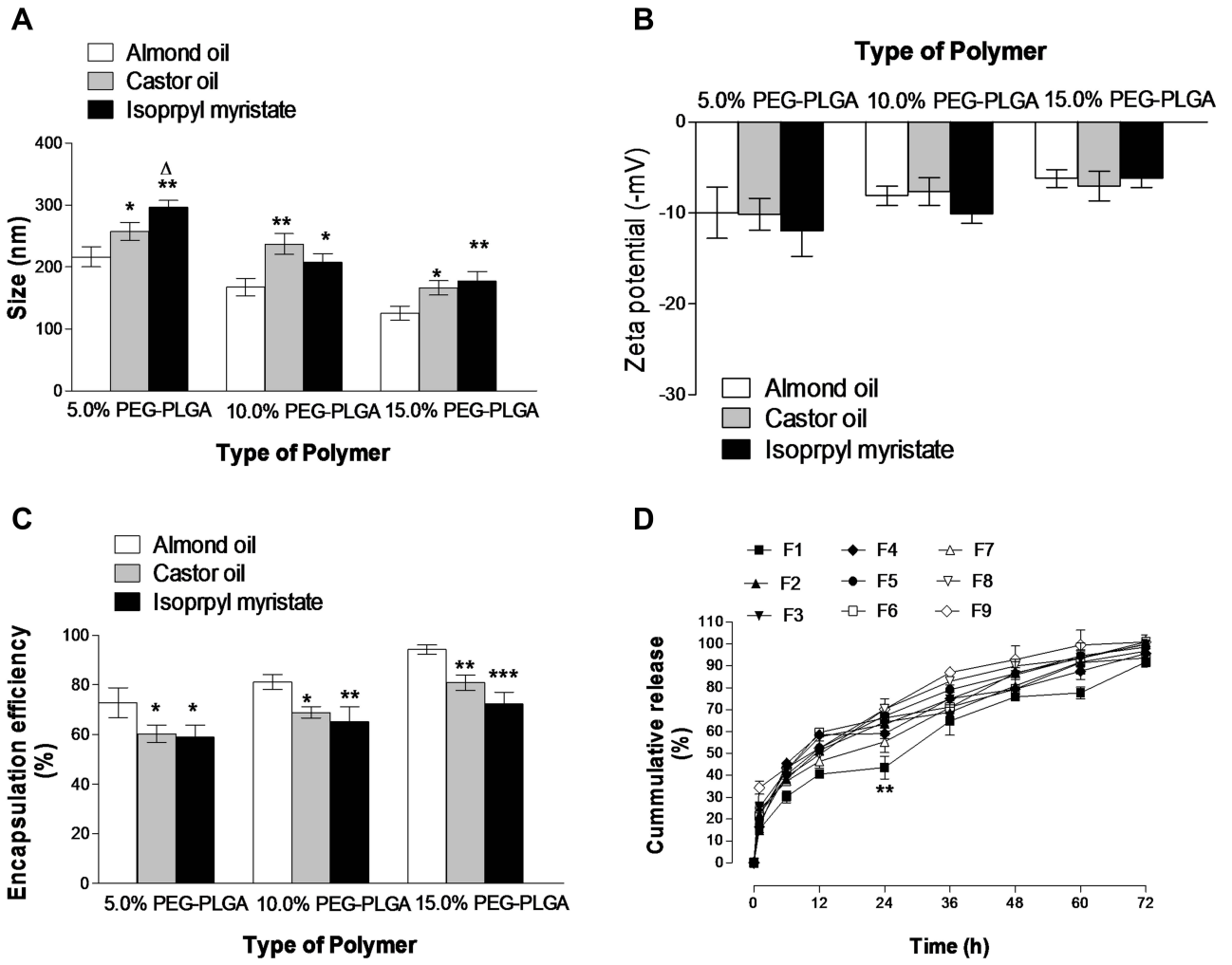

Figure 2 Effects of the type of oily core on NCs size (**A**), zeta potential (**B**), encapsulation efficiency (**C**) and HK in vitro release (**D**). Values are mean ± SD for (n = 3). For (**A**–**C**), *p < 0.05, **p < 0.01, ***p < 0.001 compared with almond oil for each polymer type. $^{\Delta}$p < 0.05 compared with castor oil for each polymer type.

In vitro release profiles showed that different oily core significantly affected the initial burst release from different polymers (Figure 2D). Lower burst release had been observed from F1, F4, and F7 (prepared from almond oil) compared to other HK-loaded NCs prepared from castor oil or isopropyl myristate. F1 with almond oily core showed a significantly lower burst release of 43.53% compared to 65.34% and 63.23% from F2 and F3 prepared from castor oil and isopropyl myristate, respectively ($p < 0.01$, n=3). Similar results were observed in the case of HK-loaded NCs prepared from 15% PEG-PLGA polymer. F7 prepared with almond oil showed a significantly lower burst release of 55.24% compared to 70.55% and 76.49% from F8 and F9 prepared from castor oil and isopropyl myristate, respectively ($p < 0.05$, n=3). This might be attributed to different polymer solubility in different oils used. 15% PEG-PLGA copolymer has lower solubility in almond oil compared to other PEGylated polymers. This lower solubility led to shorter solidification time and, consequently, leads to the formation of more dense NC structure slowing drug release.[11] These results support the higher percentage of HK entrapment in the case of NCs prepared from 15% PEG-PLGA and almond oil due to the same reasons.

Transmission Electron Microscopy

Transmission electron micrograph of F7 was represented in (Figure 3). HK-loaded NCs showed a smooth spherical surface with a narrow size distribution. The average size and size distribution obtained from TEM was comparable to what obtained from Nanosizer.

In vitro Stability

Lyophilization was used to increase the long-term storage stability of HK-loaded NCs. In vitro stability results of three different HK-loaded NCs (F1, F4, and F7) are

reported in Table 2. A slight non-significant increase in size, PDI ($p > 0.05$, n=3) meanwhile a slight decrease in zeta potential and %E.E ($p > 0.05$, n=3) after 4 and 6 months was observed. This can be attributed to the role of PEG coat in stabilizing HK-loaded NCs and improving its aqueous solubility as previously reported.[19,43] In addition, solidification of HK-loaded NCs by freeze-drying resulted in the stabilizing of HK-loaded NCs physio-chemical properties for 6 months after preparation.

Cellular Uptake of HK-Loaded NCs

This study aims to investigate the efficiency of cellular uptake of HK-loaded PEGylated PLGA NCs into MCF-7 breast cancer cells. In vitro, cellular uptake results are shown in (Figures 4 and 5). The quantitative flow cytometry analysis, which reflected the presence of the coumarin 6 tagged HK-loaded NCs in MCF-7 cells after 24 hrs of treatment, is shown in (Figure 4). The percentage of cells with positive staining following treatment with 15% PEGylated NCs was significantly higher ($p < 0.01$, n=3) than all other NP formulations made from 5% PEG-PLGA and 10% PEG-PLGA. F7 showed higher cellular uptake with 71.42% ± 6.94% positive cells, compared to 34.75% ± 4.91% and 54.81% ± 8% in the case of F1 and F4, respectively. Flow cytometry results were presented in (Supplementary Figure 1). These results showed that F7, with the lowest particle size of (125.5 ± 11.5), lowest zeta potential of (−6.21 ± 0.97 mV) and highest PEG content gave rise to the greatest uptake by MCF-7 breast cancer cells. 15% PEGylated PLGA NCs showed significantly higher cellular uptake when compared to 5% and 10% PEG-PLGA NCs, due to PEGylation pronounced effect on decreasing nanoparticles size and negative zeta potential. This suggests that particle size and zeta potential are considered to be the key determinant factors of cellular uptake.[11,44]

Confocal scanning microscopy images confirmed that F7 exhibited the largest uptake by MCF-7 cells (Figure 5). HK-loaded NCs (F7) were primarily localized in the cytoplasm, while some fluorescence intensity was observed around the nucleus (Figure 5G–I). This confirms sub-cellular drug delivery of honokiol-loaded NCs (F7) that will release HK from the biodegradable nanocapsule into the cancer cells. The coumarin 6 solution uptake by MCF-7 cells showed minimum cellular uptake (Figure 5D–F). Confocal laser microscopy images of F1 and F4 were represented in (Supplementary Figure 2). Based on these quantitative and qualitative results, it is clear that 15% PEGylated PLGA NP showed maximum cellular uptake due to optimum physio-chemical properties. Therefore, F7 was selected for further in vitro and in vivo studies due to its superior physicochemical properties and enhanced cellular uptake into breast cancer cells.

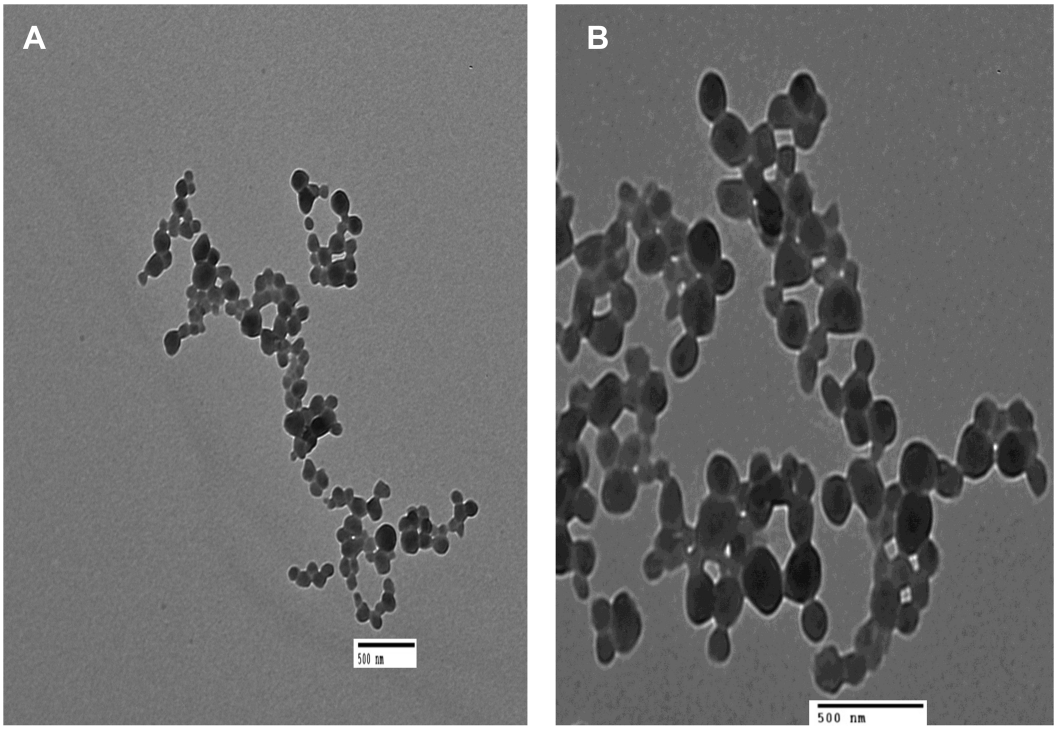

Figure 3 TEM images of HK NCs (F7) after preparation, (**A**) Mag x1000 and (**B**) Mag x2000.

Table 2 In vitro Stability Results of HK-Loaded NCs

Formulation Identifier	Time (Month)	Size (nm)	PDI	ζ-Potential (mV)	% E.E
F1	0	216.52 ± 15.95	0.21 ± 0.05	−9.97 ± 2.81	72.89 ± 6.01
	2	225.57 ± 13.71	0.23 ± 0.04	−9.52 ± 2.52	70.11 ± 5.69
	4	237.41 ± 20.11	0.22 ± 0.07	− 8.17 ± 3.19	66.89 ± 8.77
	6	247.22 ± 17.32	0.25 ± 0.06	−9.18 ± 4.42	65.22 ± 6.01
F4	0	167.51 ± 14.43	0.28 ± 0.04	−8.11 ± 1.04	81.19 ± 3.02
	2	181.42 ± 11.99	0.29 ± 0.07	−7.22 ± 2.13	77.59 ± 5.22
	4	201.75 ± 16.18	0.28 ± 0.06	−7.99 ± 1.46	75.15 ± 3.66
	6	209.31 ± 19.25	0.3 ± 0.05	−7.01 ± 1.69	74.66 ± 5.12
F7	0	125.12 ± 11.51	0.19 ± 0.06	− 6.21 ± 0.97	94.18 ± 1.82
	2	128.72 ± 19.61	0.24 ± 0.02	−5.76 ± 1.29	92.88 ± 3.12
	4	137.44 ± 16.28	0.23 ± 0.03	−6.19 ± 2.47	90.77 ± 2.24
	6	147.39 ± 14.22	0.25 ± 0.07	−5.89 ± 3.68	88.5 ± 6.72

Note: All results are presented as mean ± SD with n=3.

In vitro Cytotoxicity of HK-Loaded NCs

The anti-proliferative action of HK-loaded NCs (F7) on the MCF-7 cell line was estimated by MTT assay for 24, 48 and 72 hrs after treatment at 5, 10 and 20 µM of free honokiol and HK-loaded NCs (Figure 6). The dose–effect curves were plotted to measure the drug concentration that caused 50% growth inhibition (IC_{50}) using GraphPad Prism® software. To calculate IC_{50}, a series of different drug concentrations that resulted in different growth inhibition values were plotted as a linear standard curve (Log value of drug concentrations vs % growth inhibition). The linear regression equation of the dose–effect curve was used to calculate the IC_{50}.[20] The results showed that the blank NCs had no cytotoxicity on breast cancer cells. Treatment with honokiol showed a significant reduction in cell viability compared to control ($p < 0.05$, n=3). Free HK showed a dose-dependent cytotoxic action as cell viability decreased with increasing the dose from 5 to 20 µM. Treatment with HK-loaded NCs (F7) reduced cell viability in a dose-dependent manner meanwhile it maintained its cytotoxic action up to three days after treatment due to sustained cytotoxic action (Figure 6A). After 24 hrs of treatment, the mean IC_{50} value of HK-loaded NCs (F7) in MCF-7 cells was approximately 20 ± 2.3 µM, which is significantly lower than calculated IC_{50} of free honokiol (52.63 ± 5.4 µM) ($p < 0.001$, n=3). The mean IC50 value for HK-loaded NCs (F7) in EAC cells was approximately 10 µM, compared to 27.7 µM of free honokiol which was achieved within 3 hrs ($p < 0.001$, n=3) (Figure 6B). Based on these results, HK-loaded NCs (F7) achieved significant cytotoxic action compared to free HK due to successful HK delivery to the subcellular site of action[2] meanwhile preserving its anti-cancer activity after formulation.

In vivo Anti-Tumor Activity

In the present study, we investigated for the first time the in vivo effects of HK and HK-loaded PEG-PLGA NCs on

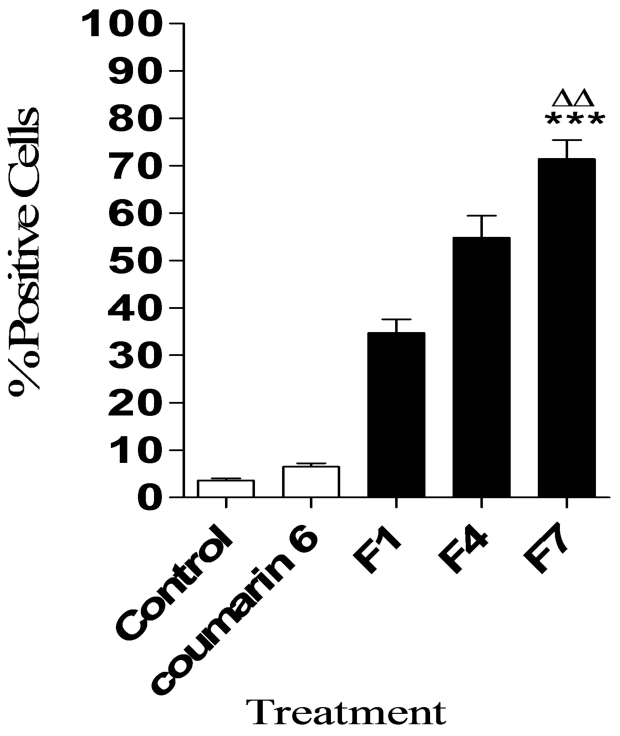

Figure 4 Quantitative cellular uptake of different types of HK NCs (F1, F4, and F7) determined by flow cytometry after 24 hrs of treatment. Results are represented as the percentage of positive cells showing cellular uptake of each NC. Values are mean ± SD for (n = 3). ***$p < 0.001$ compared with control, coumarin 6 and F1 groups. $^{\Delta\Delta}p < 0.001$ compared with F4.

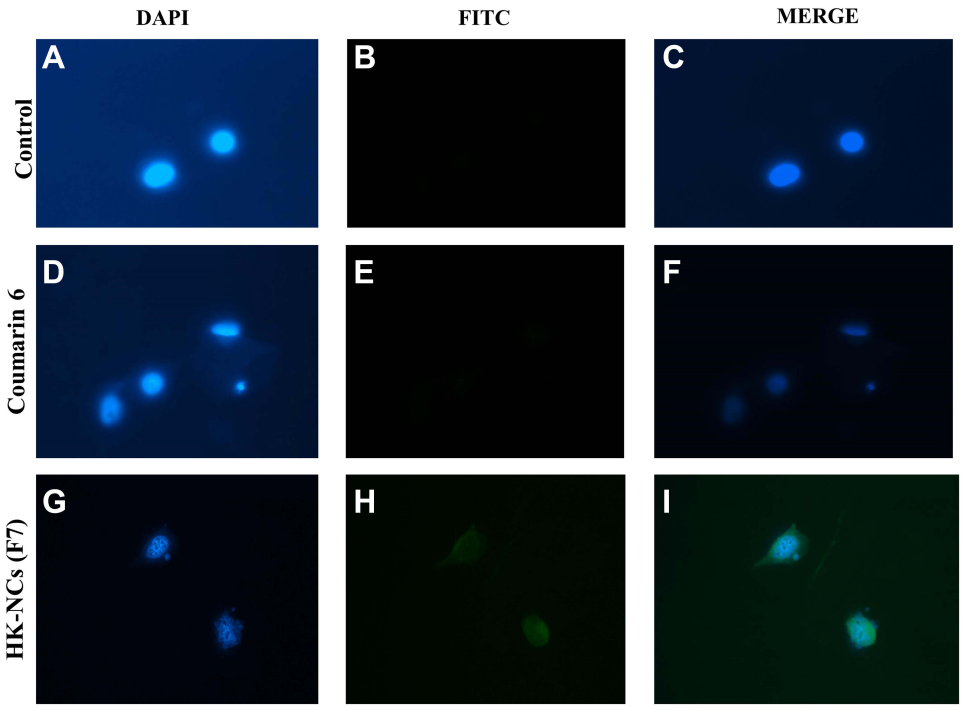

Figure 5 Confocal laser scanning microscopy images of MCF-7 control cells (**A**–**C**), cells treated with coumarin 6 (**D**–**F**) and coumarin 6 tagged HK NC (F7) (**G**–**I**) after 24 hrs of treatment.

the proliferation of SEC cells in SEC tumor-bearing mice. Solid Ehrlich Carcinoma (SEC) xenograft model is a well-established in vivo model in mice. It was commonly used to study the effect of different chemotherapeutic drugs on the treatment of breast cancer.[45] This model reflects high-grade malignancy due to its high virulence ability, infiltrative nature, and quick development.[46] Therefore, the SEC model is used to study the anti-cancer effect of HK against breast cancer after systemic administration in vivo.

The in vivo anti-tumor activity in mice-bearing SEC tumors after treatment with HK was measured by the tumor growth inhibition effect (Figure 7). After 11 days of HK treatment, the size of tumor mass in animals treated with F7 was significantly lower compared to the free drug-treated group and the control group ($p < 0.05$, n=8). Animals treated with HK solution, at a dose of (15 mg kg^{-1}) showed that HK was efficient in restraining further tumor growth after 11th day and a non-significant increase in tumor size was observed ($p > 0.05$, n=8). The average tumor size of animals treated with free HK at the end of the treatment was found to be 906.75 ± 105.32 mm^3 (Figure 7A) and the percentage tumor growth inhibition (% TGI) was approximately 35% (Figure 7B). A more pronounced effect was noticed in animals treated with HK-loaded 15% PEG-PLGA NCs. A sharp decrease in tumor size was observed starting from the 11th day of treatment and continued at each time point until the end of the experiment ($p < 0.001$, n=8). The average size of tumor mass at the end of the treatment was found to be decreased to 266.89 ± 115.69 mm^3 and the % TGI was 80.85% (Figure 7B). It is evident that the HK-loaded NCs (F7) possessed a greater anti-tumor activity when compared to free HK due to the significant reduction in tumor size.

At the end of the treatment, all animals were sacrificed. A photograph of animals bearing a tumor at the end of the experiment was shown in (Figure 8A). The difference in tumor weights between control and treated animals was exhibited in (Figure 8B). The average tumor weight in the control group after treatment was 2.16 ± 0.55 g. Animals treated with free drug, the average tumor weight was decreased to 1.2 ± 0.29 g with a percentage reduction of 45%. On the other hand, the mean tumor weight of animals treated with F7 was 0.315 ± 0.14 g. The percentage reduction in tumor weights was 85.5% which is statistically significant compared to free drug-treated mice ($p < 0.001$, n=8). The drug dose used for this study was (15 mg kg^{-1}) which is significantly lower than other published doses for similar in vivo work.[2,24]

Tumor Growth Biomarkers

Previous studies have proven that the anti-cancer activity of HK is directly related to its role in regulating various

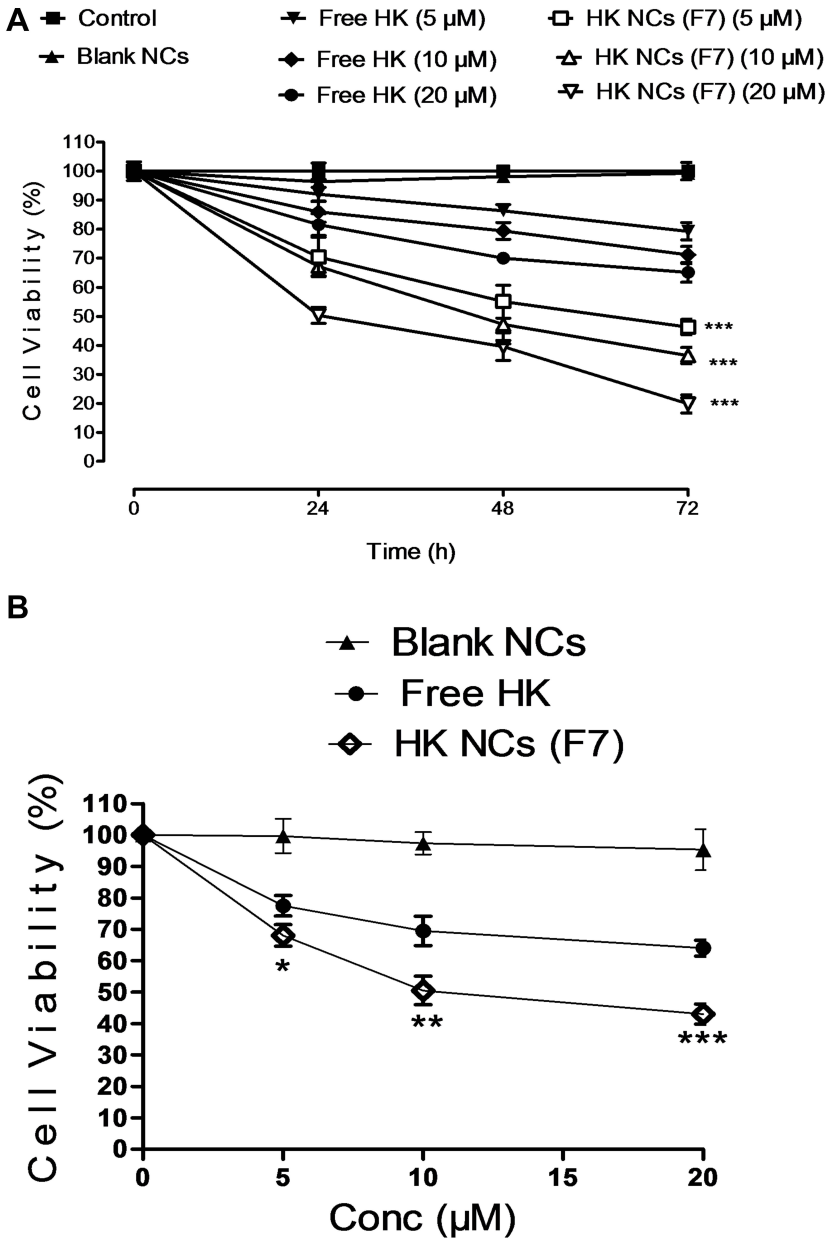

Figure 6 Cell viability results of different doses of free HK and HK NCs (F7) after 24, 48 and 72 hrs using MCF-7 cell line (**A**) and EAC cell line (**B**). Values are expressed as mean ± SD for (n = 3). For (**A** and **B**) *p < 0.05, **p < 0.01, ***p < 0.001 compared with free HK of the same dose.

signaling pathways. These include the upregulation of epithelial tumor markers and downregulation of mesenchymal tumor markers leading to apoptosis. Additionally, HK possesses an anti-metastatic effect through inhibition of angiogenesis (via the down-regulation of VEGF), invasion and migration.[2] Three different tumor markers were used in this study. Tumor growth biomarker results were represented in (Figure 9). VEGF-1 is one of the most important angiogenic factors, which mediate the formation of new blood and lymphatic vessels. It was clear from ELISA results that HK-loaded NCs (F7) exhibited a high antiangiogenic activity as it showed a significant decrease in VEGF-1 level in tumor tissue compared to control animals and free HK treated group ($p < 0.001$, n=8). Honokiol causes blockade of VEGF receptor 2 autophosphorylation and hence interfering with Rac activation which is mandatory for VEGF-induced endothelial migration and proliferation. This can explain the potential honokiol anti-angiogenic role in cancer cells.[47] Apoptosis is a form of programmed cell death that is precisely regulated. It is one of the most important types of

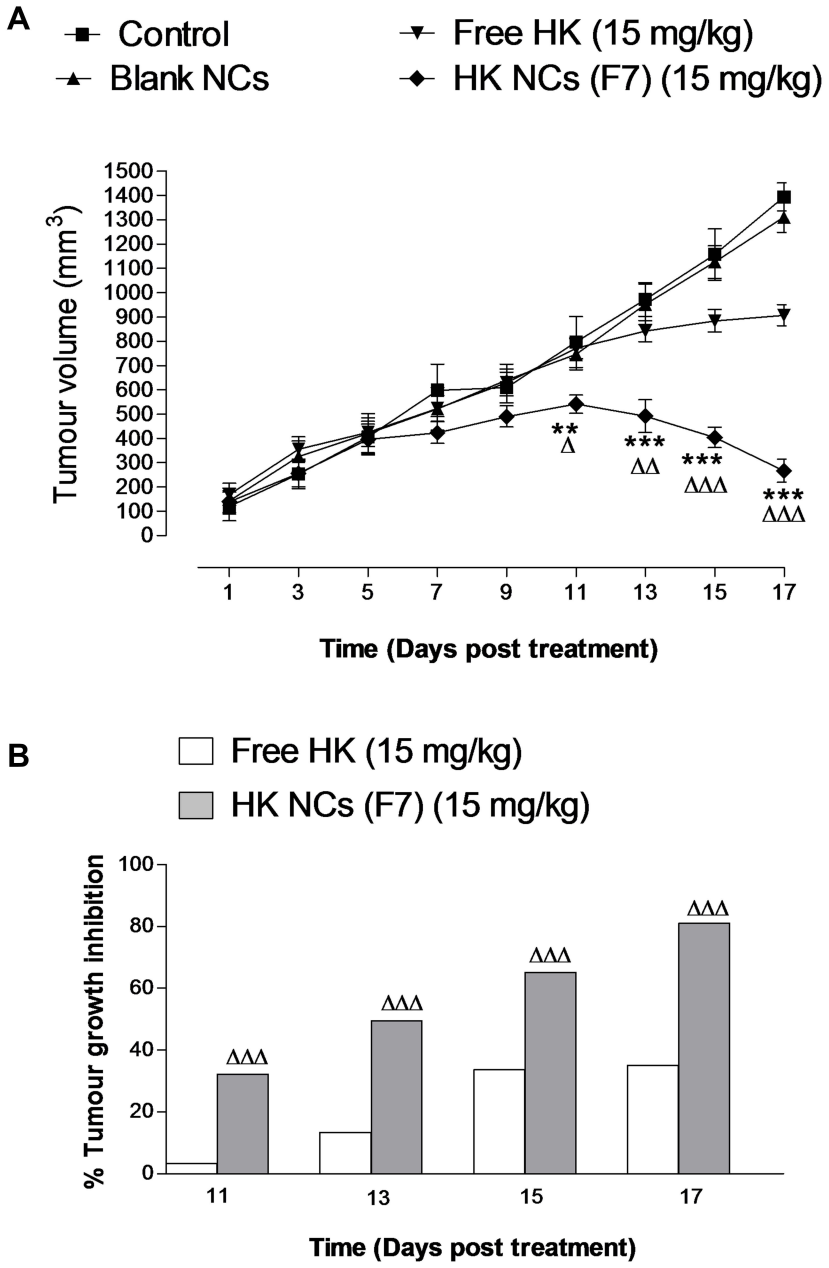

Figure 7 Tumor volume recorded for the studied animal groups every 2 days from the 1st day of the treatment to the last record on the 17th day (the end of the experiment). Values are mean ± SEM for (n = 8). **P<0.01, ***P<0.001 compared with control group. $^{\Delta}$P<0.05, $^{\Delta\Delta}$P<0.01, $^{\Delta\Delta\Delta}$P<0.001 compared with animal treated by free HK at a dose of (15 mg kg^{-1}) (**A**). Percentage tumor growth inhibition (% TGI) in animals treated with free HK or HK NCs (F7) at a dose of (15 mg kg^{-1}) $^{\Delta\Delta\Delta}$P<0.001 compared with animals treated by free HK (**B**).

cellular biomolecular signaling pathways that participate in carcinogenesis.[48] Lack of ability to undergo apoptosis is the major cause of both tumorigenesis and tumor growth.[49] There are three well-known pro-apoptotic pathways, including the death receptor, mitochondrial, and endoplasmic reticulum enzyme pathway. The B-cell lymphoma 2 (Bcl-2) groups play a major role in the regulation of the mitochondrial pathway.[50] Caspase 3 is considered one of the key mediators of apoptosis especially in the case of breast cancer.[51] It was clear from ELISA results that HK-loaded NCs (F7) exhibited a high antiangiogenic activity as it showed a significant decrease in VEGF-1 level in tumor tissue compared to control animals and free HK treated group ($p < 0.001$, n=8). Apoptotic biomarker results showed that there is a significant increase in caspase-3 level in tumor tissue compared to control and HK treated group ($p < 0.001$, n=8). On the other hand, HK-loaded NCs (F7) showed a significant decrease in pro-apoptotic Bcl-2 level in tumor

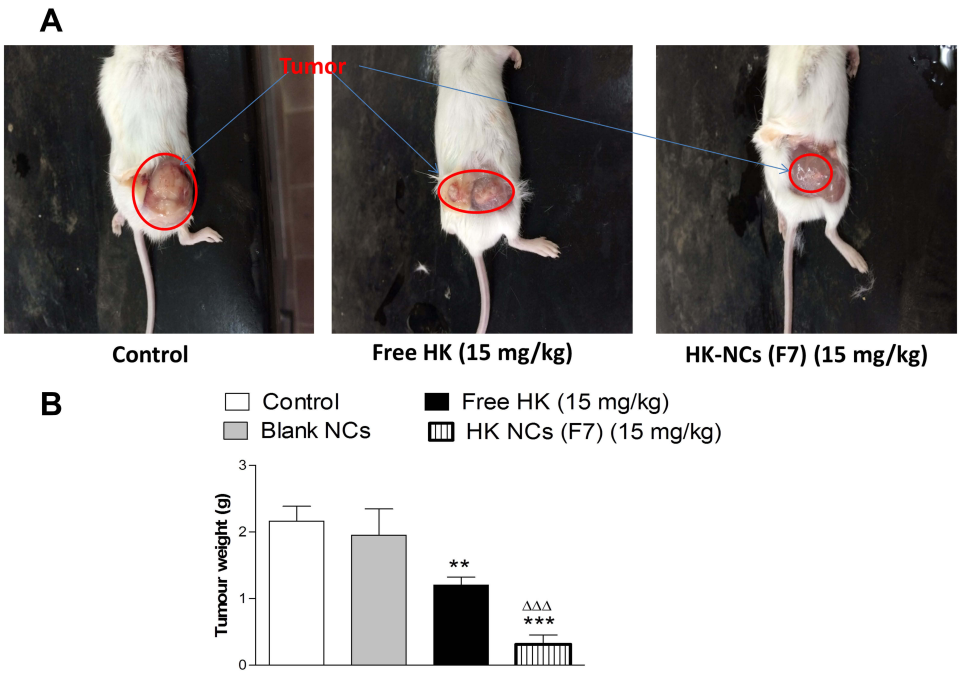

Figure 8 Photographs of control animals and animals treated with free HK and HK NCs (F7) at a dose of (15 mg kg^{-1}) (**A**). Tumor weight of studied groups after the end of the experiment. Values are mean ± SEM for (n = 8). **P<0.01, ***P<0.001 compared with control group. $^{\Delta\Delta\Delta}$P<0.001 compared with animals treated by free HK at a dose of (15 mg kg^{-1}) (**B**).

tissue homogenate ($p < 0.001$, n=8). These results confirm that HK-loaded NCs had a powerful antiangiogenic and apoptotic activity compared to free drug. Honokiol was confirmed to promote cellular apoptosis in both human and mouse malignant cells via activating caspase-3, p53/PI3K/Akt/mTOR, and ROS/ERK1/2 signaling pathway. Also, honokiol activates mitochondrial Sirt3 that disturb electron transport chain function, inducing mitochondrial fusion that enhances apoptosis.[52,53]

In vivo Safety of HK-Loaded NCs

All animals appeared healthy throughout the whole in vivo study meanwhile no substantial body weight loss was observed. There were no signs of decreased activity or abnormal behavior, which indicates no toxicity caused by treatment with either free drug or drug-loaded NCs. The measured weight gain and the immune organ index of treated and untreated mice are shown in Table 3. The body weight of all mice increased with time. The weight gain of control mice was about 3.3 ± 0.99 g. Animals treated with free HK and HK-loaded NCs (F7) showed a non-significant increase in weight gain (Figure 10). Honokiol was reported to have a non-significant effect on the normal growth and development of mice. Treatment of mice with HK as a chemopreventive agent against cancer showed a non-significant effect on weight gain.[54] Its action as non-adipogenic PPARγ agonist significantly suppressed weight gain only in diabetic mice.[8] Moreover, animals' treated groups showed a non-significant difference in immune organ index compared to control mice ($p > 0.05$, n=8). It is clear that the liver and the kidney are the most important organs for the metabolism and elimination of drugs in the body, and it is also the most vulnerable organs to damage by drug-induced effects. Therefore, biochemical assays were also used to ensure the safety of HK treatment. The effect of free HK and HK-loaded NCs (F7) on liver and kidney functions is reordered in Table 4. Extensive tissue injury resulted in the release of ALT and AST into the blood. Liver injury is associated with elevated levels of ALT. All treated animals exhibited no significant effect in ALT and AST levels in the serum samples compared with the control group ($p > 0.05$, n=8). On the other hand, kidney function measured by serum creatinine level demonstrated a non-significant increase in animal treated groups compared with control animals ($p > 0.05$). Therefore, it can be concluded that HK-loaded NCs were clearly safe after systemic administration of a dose of 15mg kg^{-1} by intraperitoneal injection.

The major challenge of anti-cancer therapeutics is to reach their predetermined cellular and subcellular target sites, meanwhile minimizing their action at nonspecific sites. Herein, surface modification of HK-loaded NCs

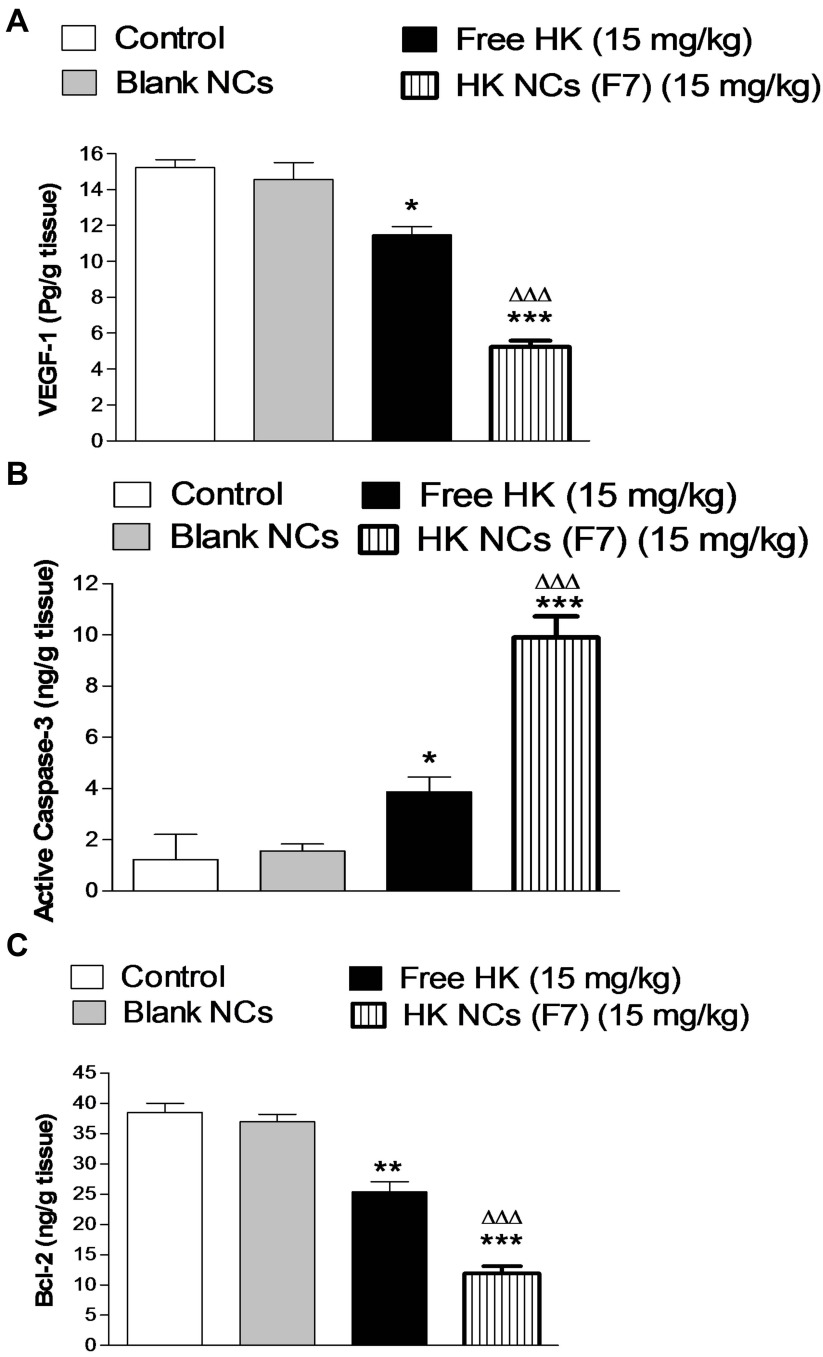

Figure 9 Tumor growth biomarkers of studied groups after the end of the experiment, VEGF-1 (**A**), Caspase-3 (**B**) and Bcl-2 (**C**). Values are mean ± SEM for (n = 8). *P<0.05, **P<0.01, ***P<0.001 compared with control group. $^{\Delta\Delta\Delta}$P<0.001 compared with animals treated by free HK at a dose of (15 mg kg^{-1}).

with polyethylene glycol (PEG) was adopted as a strategy to prolong circulation time, minimize non-specific uptake, and facilitate specific passive tumor-targeting through the well-known enhanced permeability and retention effect (EPR). The rapid uptake of PLGA nano-systems by the reticuloendothelial system, mainly by the aid of liver and spleen macrophages would be significantly decreased by modifying their surface with polyethylene glycol (PEG).[12,55] The presence of PEG chains on the surface can protect HK-loaded NCs from capture by macrophages improves its sub-cellular delivery and hence maximize its anti-cancer activity.

Conclusion

The novelty of this piece of work depends on two aspects; the use of biocompatible PEGylated PLGA oil-cored

Table 3 Effect of HK-Loaded NCs on the Immune Organ Index in Mice

Animal Group	Organ Index (mg/kg)				
	Heart	Lung	Liver	Kidneys	Spleen
Control	3.54 ± 0.23	4.21 ± 0.28	6.94 ± 0.55	7.29 ± 0.17	2.11 ± 0.25
Blank NCs	3.14 ± 0.66	4.11 ± 0.66	6.77 ± 0.11	7.51 ± 0.29	1.99 ± 0.77
Free HK (15 mg kg^{-1})	3.94 ± 0.11	4.01 ± 0.58	6.54 ± 0.93	7.44 ± 0.22	2.22 ± 0.19
HK-loaded NCs (F7) (15 mg kg^{-1})	3.12 ± 0.74	4.01 ± 0.32	7.04 ± 0.25	7.08 ± 0.27	1.89 ± 0.95

Note: Values are represented as mean ± SEM with n=8.

Table 4 Effect of HK-Loaded NCs on the Serum Level of Blood Biochemical Parameters

Animal Group	ALT (Units L^{-1})	AST (Units L^{-1})	Serum Creatinine (mg dL^{-1})
Control	18.55 ± 4.12	37.58 ± 6.47	0.49 ± 0.26
Blank NCs	16.43 ± 5.36	41.16 ± 7.53	0.57 ± 0.08
Free HK (15 mg kg^{-1})	21.91 ± 2.77	37.16 ± 10.99	0.56 ± 0.44
HK-loaded NCs (F7) (15 mg kg^{-1})	20.95 ± 6.55	42.36 ± 8.68	0.48 ± 0.99

Note: Values are represented as mean ± SEM with n=8.

nanocapsules for honokiol loading, and in vivo application of optimum HK-loaded NCs for breast cancer treatment using SEC model. In an attempt to optimize the formulation of HK-loaded NCs, different PEG-PLGA diblock copolymers and different types of oily core were studied. Optimum HK-loaded NCs were prepared from 15% PEG-PLGA with the smallest size, narrow polydispersity index, highest drug loading and highest cellular uptake by MCF-7 breast cancer cells compared with other HK-loaded NCs. Optimum HK-loaded NCs exhibited a significant cytotoxic action against MCF-7 and EAC breast cancer cells due to their lower IC_{50} compared to free HK. Moreover, in vivo results supported the enhanced anti-tumor activity of HK-loaded NCs as approximately 80% reduction in tumor growth and 85% inhibition in tumor weight were observed after treatment with HK-loaded NCs. HK-NCs successfully inhibited angiogenesis and enhanced apoptosis as assessed by tumor growth biomarkers. The PEGylated nanocapsule drug delivery system was found to be safe in vivo after systemic administration to mice-bearing tumors as indicated by immune organ index and biochemical analysis. In conclusion, our results clearly indicate that HK-loaded PEGylated NCs are a promising anticancer agent, to treat breast carcinogenesis.

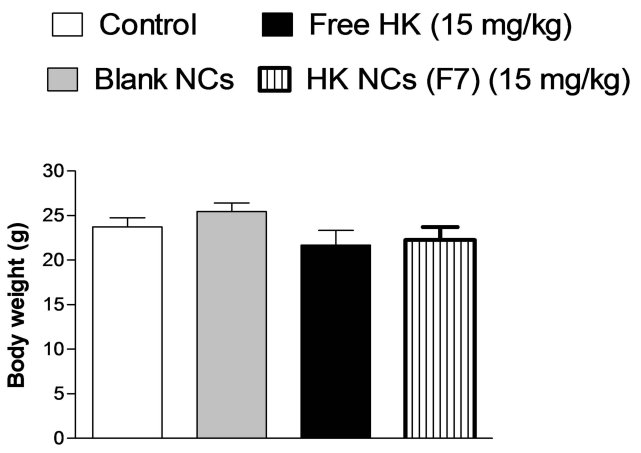

Figure 10 Bodyweight of studied animal groups treated with free HK and HK NCs (F7) at a dose of (15 mg kg^{-1}) after the end of the experiment, Values are mean ± SEM for (n = 8).

Disclosure

We declare no financial or personal relationships with other people or organizations that could inappropriately affect this study. There are no competing interests in this work.

References

1. Siegel RL, Miller KD, Jemal A. Cancer statistics, 2019. *CA Cancer J Clin*. 2019;69(1):7–34. doi:10.3322/caac.21551
2. Nagalingam A, Arbiser JL, Bonner MY, Saxena NK, Sharma D. Honokiol activates AMP-activated protein kinase in breast cancer cells via an LKB1-dependent pathway and inhibits breast carcinogenesis. *Breast Cancer Res*. 2012;14(1):R35. doi:10.1186/bcr3128
3. Lee YJ, Lee YM, Lee CK, Jung JK, Han SB, Hong JT. Therapeutic applications of compounds in the Magnolia family. *Pharmacol Ther*. 2011;130(2):157–176. doi:10.1016/j.pharmthera.2011.01.010
4. Liou K-T, Shen Y-C, Chen C-F, Tsao C-M, Tsai S-K. The anti-inflammatory effect of honokiol on neutrophils: mechanisms in the inhibition of reactive oxygen species production. *Eur J Pharmacol*. 2003;475(1–3):19–27. doi:10.1016/S0014-2999(03)02121-6
5. Lo Y-C, Che-ming T, Chieh-fu C, Chien-chih C, Chuang-ye H. Magnolol and honokiol isolated from Magnolia officinalis protect rat heart mitochondria against lipid peroxidation. *Biochem Pharmacol*. 1994;47(3):549–553. doi:10.1016/0006-2952(94)90187-2
6. Liou K-T, Lin S-M, Huang -S-S, Chih C-L, Tsai S-K. Honokiol ameliorates cerebral infarction from ischemia-reperfusion injury in rats. *Planta Med*. 2003;69(2):130–134. doi:10.1055/s-2003-37707
7. Maruyama Y, Kuribara H. Overview of the pharmacological features of honokiol. *CNS Drug Rev*. 2000;6(1):35–44. doi:10.1111/j.1527-3458.2000.tb00136.x

8. Atanasov AG, Wang JN, Gu SP, et al. Honokiol: a non-adipogenic PPARγ agonist from nature. *Biochim Biophys Acta*. 2013;1830 (10):4813–4819. doi:10.1016/j.bbagen.2013.06.021
9. Natarajan JV, Nugraha C, Ng XW, Venkatraman S. Sustained-release from nanocarriers: a review. *J Control Release*. 2014;193:122–138. doi:10.1016/j.jconrel.2014.05.029
10. Haggag Y, Abdel-wahab Y, Ojo O, et al. Preparation and in vivo evaluation of insulin-loaded biodegradable nanoparticles prepared from diblock copolymers of PLGA and PEG. *Int J Pharm*. 2016;499(1–2):236–246. doi:10.1016/j.ijpharm.2015.12.063
11. Haggag YA, Matchett KB, Dakir El H, et al. Nano-encapsulation of a novel anti-Ran-GTPase peptide for blockade of regulator of chromosome condensation 1 (RCC1) function in MDA-MB-231 breast cancer cells. *Int J Pharm*. 2017;521(1–2):40–53. doi:10.1016/j.ijpharm.2017.02.006
12. Haggag YA, Osman MA, El-gizawy SA, et al. Polymeric nano-encapsulation of 5-fluorouracil enhances anti-cancer activity and ameliorates side effects in solid Ehrlich Carcinoma-bearing mice. *Biomed Pharmacother*. 2018;105:215–224. doi:10.1016/j.biopha.2018.05.124
13. Drozdek S, Bazylińska U. Biocompatible oil core nanocapsules as potential co-carriers of paclitaxel and fluorescent markers: preparation, characterization, and bioimaging. *Colloid Polym Sci*. 2016;294:225–237. doi:10.1007/s00396-015-3767-5
14. Klippstein R, Wang JT, El-gogary RI, et al. Passively targeted curcumin-loaded PEGylated PLGA nanocapsules for colon cancer therapy in vivo. *Small*. 2015;11(36):4704–4722. doi:10.1002/smll.201403799
15. Szczepanowicz K, Bazylinska U, Pietkiewicz J, Szyk-warszynska L, Wilk KA, Warszynski P. Biocompatible long-sustained release oil-core polyelectrolyte nanocarriers: from controlling physical state and stability to biological impact. *Adv Colloid Interface Sci*. 2015;222:678–691. doi:10.1016/j.cis.2014.10.005
16. Bazylińska U, Lewińska A, Lamch Ł, Wilk KA. Polymeric nanocapsules and nanospheres for encapsulation and long sustained release of hydrophobic cyanine-type photosensitizer. *Colloids Surf a Physicochem Eng Asp*. 2014;442:42–49. doi:10.1016/j.colsurfa.2013.02.023
17. Hu C, Chen Z, Wu S, et al. Micelle or polymersome formation by PCL-PEG-PCL copolymers as drug delivery systems. *Chin Chem Lett*. 2017;28(9):1905–1909. doi:10.1016/j.cclet.2017.07.020
18. Haggag YA, Faheem AM, Tambuwala MM, et al. Effect of poly (ethylene glycol) content and formulation parameters on particulate properties and intraperitoneal delivery of insulin from PLGA nanoparticles prepared using the double-emulsion evaporation procedure. *Pharm Dev Technol*. 2018;23(4):370–381. doi:10.1080/10837450.2017.1295066
19. Haggag YA, Faheem AM. Evaluation of nano spray drying as a method for drying and formulation of therapeutic peptides and proteins. *Front Pharmacol*. 2015;6:140. doi:10.3389/fphar.2015.00140
20. Haggag YA, Matchett KB, Falconer RA, et al. Novel ran-RCC1 inhibitory peptide-loaded nanoparticles have anti-cancer efficacy in vitro and in vivo. *Cancers*. 2019;11(2):222. doi:10.3390/cancers11020222
21. Han M, Yu X, Guo Y, Wang Y, Kuang H, Wang X. Honokiol nanosuspensions: preparation, increased oral bioavailability and dramatically enhanced biodistribution in the cardio-cerebro-vascular system. *Colloids Surf B Biointerfaces*. 2014;116:114–120. doi:10.1016/j.colsurfb.2013.12.056
22. Zheng X, Kan B, Gou M, et al. Preparation of MPEG-PLA nanoparticle for honokiol delivery in vitro. *Int J Pharm*. 2010;386(1–-2):262–267. doi:10.1016/j.ijpharm.2009.11.014
23. Tang P, Sun Q, Yang H, Tang B, Pu H, Li H. Honokiol nanoparticles based on epigallocatechin gallate functionalized chitin to enhance therapeutic effects against liver cancer. *Int J Pharm*. 2018;545 (1):74–83. doi:10.1016/j.ijpharm.2018.04.060
24. Wu W, Wang L, Wang L, et al. Preparation of honokiol nanoparticles by liquid antisolvent precipitation technique, characterization, pharmacokinetics, and evaluation of inhibitory effect on HepG2 cells. *Int J Nanomedicine*. 2018;13:5469–5483. doi:10.2147/IJN.S178416
25. Wu Q, Zhang M, Luo H, Yi T. Self-assembled honokiol-loaded microbubbles in the treatment of ovarian cancer by ultrasound irradiation. *J Biomed Nanotechnol*. 2018;14(10):1796–1805. doi:10.1166/jbn.2018.2628
26. Wang X-H, Cai -L-L, Zhang X-Y, et al. Improved solubility and pharmacokinetics of PEGylated liposomal honokiol and human plasma protein binding ability of honokiol. *Int J Pharm*. 2011;410 (1):169–174. doi:10.1016/j.ijpharm.2011.03.003
27. Gou M, Zheng X, Men K, et al. Self-assembled hydrophobic honokiol loaded MPEG-PCL diblock copolymer micelles. *Pharm Res*. 2009;26(9):2164–2173. doi:10.1007/s11095-009-9929-8
28. Qiu N, Cai LL, Xie D, et al. Synthesis, structural and in vitro studies of well-dispersed monomethoxy-poly(ethylene glycol)-honokiol conjugate micelles. *Biomed Mater*. 2010;5(6):065006. doi:10.1088/1748-6041/5/6/065006
29. AbdElhamid AS, Zayed DG, Helmy MW, et al. Lactoferrin-tagged quantum dots-based theranostic nanocapsules for combined COX-2 inhibitor/herbal therapy of breast cancer. *Nanomedicine (Lond)*. 2018;13(20):2637–2656. doi:10.2217/nnm-2018-0196
30. Abdelmoneem MA, Elnaggar MA, Hammady RS, et al. Dual-targeted lactoferrin shell-oily core nanocapsules for synergistic targeted/herbal therapy of hepatocellular carcinoma. *ACS Appl Mater Interfaces*. 2019;11(30):26731–26744. doi:10.1021/acsami.9b10164
31. Fessi H, Puisieux F, Devissaguet JP, Ammoury N, Benita S. Nanocapsule formation by interfacial polymer deposition following solvent displacement. *Int J Pharm*. 1989;55(1):R1–R4. doi:10.1016/0378-5173(89)90281-0
32. Ahmed O, Ahmed R. Anti-proliferative and apoptotic efficacies of ulvan polysaccharides against different types of carcinoma cells in vitro and in vivo. *J Cancer Sci Ther*. 2014;6:202–208. doi:10.4172/1948-5956.1000272
33. Ahmed OM, Ahmed RR. Anti-proliferative and apoptotic efficacy of diallyl disulfide on Ehrlich ascites carcinoma. *Hepatoma Res*. 2015;1 (2):67–74. doi:10.4103/2394-5079.157602
34. Papadopoulos D, Kimler BF, Estes NC, Durham FJ. Growth delay effect of combined interstitial hyperthermia and brachytherapy in a rat solid tumor model. *Anticancer Res*. 1989;9(1):45–47.
35. BassiouniSanceau J, Poupon MF, Delattre O, Sastre-garau X, Wietzerbin J. Strong inhibition of Ewing tumor xenograft growth by combination of human interferon-alpha or interferon-beta with ifosfamide. *Oncogene*. 2002;21(50):7700–7709. doi:10.1038/sj.onc.1205881
36. Mora-huertas CE, Fessi H, Elaissari A. Polymer-based nanocapsules for drug delivery. *Int J Pharm*. 2010;385(1–2):113–142.
37. Zhang J, Jiang W, Zhao X, Wang Y. Preparation and characterization of polymeric micelles from poly (d, l-lactide) and methoxypolyethylene glycol block copolymers as potential drug carriers. *Tsinghua Sci Technol*. 2007;12(4):493–496. doi:10.1016/S1007-0214(07)70073-1
38. Essa S, Rabanel JM, Hildgen P. Effect of polyethylene glycol (PEG) chain organization on the physicochemical properties of poly(D, L-lactide) (PLA) based nanoparticles. *Eur J Pharm Biopharm*. 2010;75(2):96–106. doi:10.1016/j.ejpb.2010.03.002
39. Khan MN, Haggag YA, Lane ME, McCarron PA, Tambuwala MM. Polymeric nano-encapsulation of curcumin enhances its anti-cancer activity in breast (MDA-MB231) and lung (A549) cancer cells through reduction in expression of HIF-1alpha and nuclear p65 (Rel A). *Curr Drug Deliv*. 2018;15(2):286–295. doi:10.2174/1567201814666171019104002
40. El-hammadi MM, Delgado AV, Melguizo C, Prados JC, Arias JL. Folic acid-decorated and PEGylated PLGA nanoparticles for improving the antitumour activity of 5-fluorouracil. *Int J Pharm*. 2017;516 (1–2):61–70. doi:10.1016/j.ijpharm.2016.11.012

41. Locatelli E, Comes Franchini M. Biodegradable PLGA-b-PEG polymeric nanoparticles: synthesis, properties, and nanomedical applications as drug delivery system. *J Nanopart Res*. 2012;14(12):1–17. doi:10.1007/s11051-012-1316-4
42. Balakumar K, Raghavan CV, Selvan NT, Prasad RH, Abdu S. Self nanoemulsifying drug delivery system (SNEDDS) of rosuvastatin calcium: design, formulation, bioavailability and pharmacokinetic evaluation. *Colloids Surf B Biointerfaces*. 2013;112:337–343. doi:10.1016/j.colsurfb.2013.08.025
43. Avgoustakis K, Beletsi A, Panagi Z, et al. Effect of copolymer composition on the physicochemical characteristics, in vitro stability, and biodistribution of PLGA-mPEG nanoparticles. *Int J Pharm*. 2003;259(1–2):115–127. doi:10.1016/S0378-5173(03)00224-2
44. Pamujula S, Hazari S, Bolden G, et al. Cellular delivery of PEGylated PLGA nanoparticles. *J Pharm Pharmacol*. 2012;64(1):61–67. doi:10.1111/j.2042-7158.2011.01376.x
45. Silva LA, Nascimento KA, Maciel MC, et al. Sunflower seed oil-enriched product can inhibit Ehrlich solid tumor growth in mice. *Chemotherapy*. 2006;52(2):91–94. doi:10.1159/000091308
46. Sakai M, Ferraz-de-paula V, Pinheiro ML, et al. Translocator protein (18 kDa) mediates the pro-growth effects of diazepam on Ehrlich tumor cells in vivo. *Eur J Pharmacol*. 2010;626(2–3):131–138. doi:10.1016/j.ejphar.2009.09.036
47. Bai X, Cerimele F, Ushio-fukai M, et al. Honokiol, a small molecular weight natural product, inhibits angiogenesis in vitro and tumor growth in vivo. *J Biol Chem*. 2003;278(37):35501–35507. doi:10.1074/jbc.M302967200
48. Wong RSY. Apoptosis in cancer: from pathogenesis to treatment. *J Exp Clin Cancer Res*. 2011;30(1):87. doi:10.1186/1756-9966-30-87
49. Wieck MM, Spurrier RG, Levin DE, et al. Sequestration of vascular endothelial growth factor (VEGF) induces late restrictive lung disease. *PLoS One*. 2016;11(2):e0148323. doi:10.1371/journal.pone.0148323
50. Wang C, Youle RJ. The role of mitochondria in apoptosis. *Annu Rev Genet*. 2009;43:95–118. doi:10.1146/annurev-genet-102108-134850
51. O'donovan N, Crown J, Stunell H, et al. Caspase 3 in breast cancer. *Clin Cancer Res*. 2003;9(2):738–742.
52. Chio CC, Chen KY, Chang CK, et al. Improved effects of honokiol on temozolomide-induced autophagy and apoptosis of drug-sensitive and -tolerant glioma cells. *BMC Cancer*. 2018;18(1):379. doi:10.1186/s12885-018-4267-z
53. Huang K, Chen Y, Zhang R, et al. Honokiol induces apoptosis and autophagy via the ROS/ERK1/2 signaling pathway in human osteosarcoma cells in vitro and in vivo. *Cell Death Dis*. 2018;9(2):157. doi:10.1038/s41419-017-0166-5
54. Chilampalli S, Zhang X, Fahmy H, et al. Chemopreventive effects of honokiol on UVB-induced skin cancer development. *Anticancer Res*. 2010;30(3):777–783.
55. van Vlerken LE, Vyas TK, Amiji MM. Poly(ethylene glycol)-modified nanocarriers for tumor-targeted and intracellular delivery. *Pharm Res*. 2007;24(8):1405–1414. doi:10.1007/s11095-007-9284-6